Magneto-optical and magnetic study of amorphous U-As, U-As-Cu, and U-As-Ti films

P. Fumagalli, T. S. Plaskett, T. R. McGuire, R. J. Gambino, and N. A. Bojarczuk
IBM Thomas J. Watson Research Center, Yorktown Heights, New York 10598
(Received 19 March 1992)

Magneto-optical and magnetic properties are presented in sputtered amorphous thin films of U-As, U-As-Cu, and U-As-Ti. Included are magnetization, Hall effect, resistivity, and polar Kerr-rotation measurements. The U-As films show maximum magnetization and Curie-temperature values at $x \simeq 57$ at. % U concentration. The largest Kerr rotation of $-2.7°$ is measured in $U_{61}As_{39}$ at 1.1 eV. The Kerr response in the U-As-Cu films is much smaller reaching $-1.05°$ at 1.05 eV in $U_{43}As_{28}Cu_{29}$. Maximum Kerr rotation in the U-As-Ti films is $-1.45°$ at 1.3 eV in $U_{42}As_{49}Ti_{09}$. At U concentrations $x < 55$ at. %, the U-As system shows phase separation into two amorphous phases, presumably a metallic UAs and a semiconducting UAs_2 phase. In the U-As-Cu system, for [U]/[As] ratio $\simeq 0.7$, magneto-optical evidence for such a phase separation is presented as well. The U-As-Ti films, however, do not show any indication of phase separation in the composition range investigated. It is concluded that the addition of Cu to U-As does not change the local coordination of the U atoms, while the addition of Ti changes the local coordination of the U atoms to a configuration as in U-As with high [U]/[As] ratios. A formula for the influence of the substrate on the Kerr rotation is derived.

INTRODUCTION

Uranium compounds are of interest because of their large magneto-optical effects. In particular, the crystalline monochalcogenides UX, where X=S,Se,Te, and monopnictides UZ, where Z=P,As,Sb, have been studied[1,2] extensively. Both systems show magnetic ordering. The monochalcogenides are ferromagnetic with a Curie temperature T_C as high as 177 K for US while the monopnictides order antiferromagnetically. Other binary crystalline compounds investigated[3,4] are the Th_3P_4-structure compounds U_3P_4 and U_3As_4, which are ferromagnets with T_C of 138 K and 198 K, respectively. We have previously reported on "giant" magnetoresistance,[5] large magneto-optical rotation,[6] and Hall effect[7] in amorphous ferromagnetic U-Sb films.

The magnetic properties of the amorphous U-As films have been published before.[8] They are ferromagnetic over a range $x \simeq 49$ to 75, where x is the concentration in at. % U. The U-As films show for $x < 55$ a phase separation into two amorphous phases which a percolation analysis suggests to be metallic UAs and semiconducting UAs_2.[9] It is known[10] that addition of Cu and Ni to uranium pnictide compounds form highly symmetric crystals of the general formula UMX_2 and UM_2X_2, where M=Cu,Ni and X=P,As. The Cu ternaries are ferromagnets with T_C reaching 216 K in UCu_2P_2, in contrast to the Ni containing compounds, which are antiferromagnets. The Cu ternaries also show large magneto-optical rotations.[11–13] The high values of T_C in these compounds give rise to questions about the underlaying mechanisms that may increase T_C in U compounds and whether it is possible to achieve a T_C above room temperature with the magnetic moment on the U atom. In order to study these mechanisms, the influence on T_C and on the magneto-optical properties of the addition of Cu to amorphous U-As films is investigated. The magnetic properties of amorphous U-As-Cu have been reported before.[14] The addition of Ti, which has a higher valence than Cu, is studied to determine the influence of additional electrons on the magnetic and magneto-optical properties. This should provide a clue if the exchange is dominated by the Ruderman-Kittel-Kasuya-Yosida (RKKY) interaction.

EXPERIMENTAL

The films are prepared by a combination of dc and rf magnetron sputtering. Layers of U (partially depleted of ^{235}U), As, and Cu or Ti of thickness between 0.5 and 1.2 Å are sequentially deposited onto glass substrates at ambient temperatures. The U, Cu, and Ti are deposited by dc and the As is deposited by rf magnetron sputtering. The base pressure is 4×10^{-8} Torr and the sputtering atmosphere is Ar at 3×10^{-3} Torr. Deposition rates are 0.5–3 Å/s and the thickness of all films is about 1500 Å. The x-ray analysis shows that the films are amorphous over the entire composition range investigated. The chemical compositions are determined by an inductively coupled plasma atomic emission-spectroscopy method and by electron-microprobe analysis.

Magnetic measurements are made using a superconducting quantum interference device (SQUID) magnetometer over a range of fields up to 4 T and temperatures of 5–260 K. In all cases, the applied magnetic field is parallel to the substrate, i.e., the field is in the plane. The number of Bohr magnetons per U atom, M_U, is calculated from magnetic moments measured in emu units and the total U content of the sample as determined from chemical analysis.

Transport measurement are done using the van der Pauw technique.[15] Pressure contacts are used except for high resistive samples where indium solder contacts are made. Hall resistivity ρ_H is obtained for fields up to 1.25 T applied perpendicular to the plane of the film. The

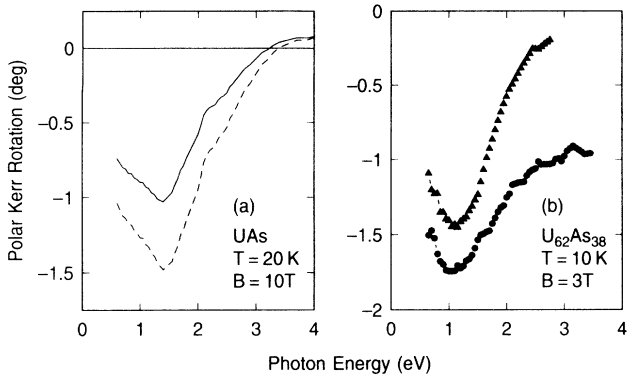

FIG. 1. (a) The polar Kerr rotation of crystalline UAs as measured on the surface (solid line; data taken from Ref. 2) and as calculated through a glass substrate with $n_s = 1.4$ (dashed line). (b) The polar Kerr rotation of an amorphous $U_{62}As_{38}$ film as measured from the film side (▲) and through a glass substrate (●).

Hall angle θ_H is given by $\theta_H = \arctan(\rho_H/\rho)$. The sample resistivity ρ is obtained by averaging voltages for adjacent contacts in the Hall setup.

The polar Kerr rotation is measured using an Oxford optical dewar with a split-coil superconducting magnet. Fields up to 7 T can be applied. A standard lock-in technique is used to determine the Kerr rotation.[2] In order to assure a clean surface, the films are measured through the substrate, which limits the photon energy range 0.65–3.5 eV. To account for the Faraday rotation of the substrate and the cryostat windows, the rotation of a gold or aluminum reference mirror is measured through the substrate and subtracted from the rotation of the sample. All energy spectra are obtained in both positive and negative magnetic fields and averaged to cancel any birefringence of nonmagnetic origin, e.g., stress-induced. The remanence spectra are obtained by field-cooling the sample in a high field prior to reducing the field to zero.

It has to be pointed out that measuring through the substrate not only limits the photon energy range but also alters the magnitude of the polar Kerr effect. The polar Kerr effect is generally enhanced by a factor equivalent to the index of refraction n_s of the substrate as derived in the Appendix. For a glass substrate this implies an overall increase of about 40%. Figure 1(a) shows the polar Kerr rotation of crystalline UAs as measured[2] on a cleaved surface (solid line) and as calculated for a glass substrate with $n_s = 1.4$ (dashed line). The spectra of an amorphous $U_{62}As_{38}$ film are plotted in Fig. 1(b) as measured from the film side (▲) and the substrate side (●), corroborating an overall enhancement of the Kerr response.

RESULTS

The magnetization per U atom M_U and the Curie temperature T_C are shown in Figs. 2 and 3, respectively, as a function of the U concentration x in the binary U-As system (left) and of the Cu or Ti concentration y in the ternary U-As-Cu and U-As-Ti system (right). The ternary

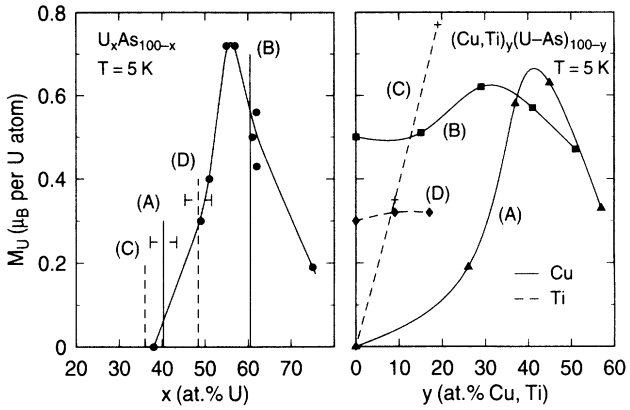

FIG. 2. The magnetization per U atom at 5 K (left) as a function of U concentration for the binary U-As system and (right) as a function of Cu and Ti concentration in the ternary U-As-Cu and U-As-Ti system keeping the ratio [U]/[As] fixed. Solid lines are to guide the eye. (A)–(D) denote the ratio [U]/[As] and are indicated as vertical lines on the left. The error bars denote the deviation in the ratio [U]/[As] where applicable. Compositions measured are [U]-[As] 38-62, 49-51, 51-49, 55-45, 57-43, 61-39, 62-38, 62-38, 75-25 at.%; (A) [U]/[As]≃0.7: U-As-Cu 16-27-57, 21-34-45, 26-37-37, 33-41-26 at.%; (B) [U]/[As]≃1.3: U-As-Cu 30-19-51, 35-23-41, 43-28-29, 51-34-15 at.%; (C) [U]/[As]≃0.5: U-As-Ti 29-52-19, 33-58-09 at.%; (D) [U]/[As]≃1: U-As-Ti 42-41-17, 42-49-09 at.%.

alloys are made in two compositional sets; in U-As-Cu alloys with an approximate ratio [U]/[As]≃0.7 (A) and [U]/[As]≃1.3 (B), in U-As-Ti alloys with [U]/[As]≃0.5 (C) and [U]/[As]≃1 (D). The binary U_xAs_{100-x} alloy is ferromagnetic in the composition range $x \simeq 49$–75 with a maximum M_U of $0.72\mu_B$ at $x \simeq 57$ (Fig. 2 left). These values are revised and differ slightly from our previous

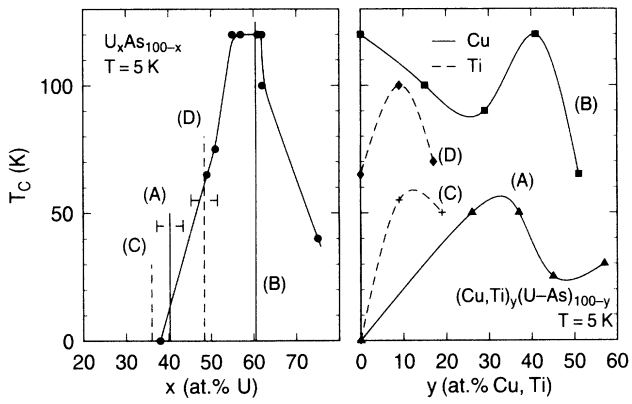

FIG. 3. The Curie temperature T_C (left) as a function of U concentration for the binary U-As system and (right) as a function of Cu and Ti concentration in the ternary U-As-Cu and U-As-Ti system keeping the ratio [U]/[As] fixed. Solid lines are to guide the eye. (A)–(D) denote the ratio [U]/[As] and are indicated as vertical lines on the left. The error bars denote the deviation in the ratio [U]/[As] where applicable. Compositions of U-As, U-As-Cu, and U-As-Ti are listed in the caption of Fig. 2.

publication.[8] The values of T_C peak between $x \simeq 55$ and $x \simeq 62$ reaching 120 K (Fig. 3 left). Adding Cu or Ti extends the ferromagnetic region down to $x < 20$ (Figs. 2 and 3 right).

For high [U]/[As] ratio (set B in Figs. 2 and 3) additions of Cu up to $y = 40\%$ in $Cu_y(U\text{-}As)_{100-y}$ do not influence M_U or T_C as compared to the binary U-As composition with the same [U]/[As] ratio. For lower [U]/[As] ratio (set A) the addition of Cu has a large enhancement effect on the magnetic properties of the films. Even at the highest Cu dopings, corresponding to U concentrations of 16 at. %, the films are still ferromagnetic. M_U and T_C peak near $y \simeq 40$. Values of M_U are as high as the highest values in U-As. T_C, on the other hand, reaches 50 K at the maximum. Adding Ti has similar effects on M_U and T_C as adding Cu. For ratio [U]/[As] $\simeq 1$ (set D in Figs. 2 and 3 right) M_U and T_C are comparable in magnitude to the U-As compositions with the same [U]/[As] ratio. For low [U]/[As] ratio (set C) M_U increases strongly as a function of Ti doping and an extension of the ordered state to low U concentrations is observed, too.

Figure 4 shows the room-temperature resistivity ρ as a function of U concentration x in the binary U-As system (left) and as function of the Cu or Ti concentration y in the ternary U-As-Cu and U-As-Ti system (right). The rapid increase in ρ towards lower U concentrations in the binary U-As system (Fig. 4 left) has been interpreted[9] as a phase separation into a metallic and a semiconducting amorphous phase. This phase separation is suppressed by the addition of Cu and Ti. For low [U]/[As] ratio (set A and C in Fig. 4 right) the resistivity decreases rapidly with increasing Cu or Ti concentration or with decreasing U concentration, whereas for high [U]/[As] ratio the resistivity stays approximately constant (set B and D).

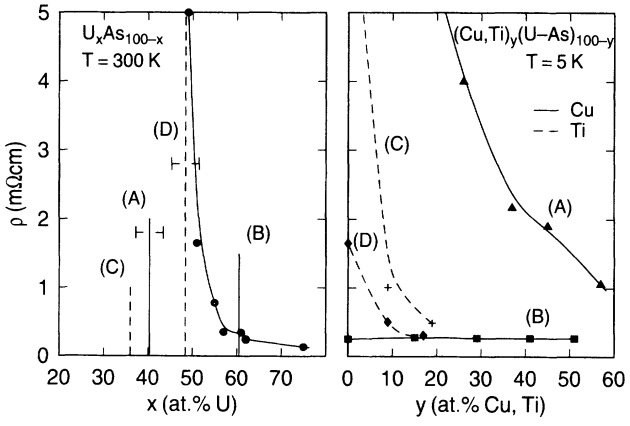

FIG. 4. The resistivity ρ at room temperature (left) as a function of U concentration for the binary U-As system and (right) as a function of Cu and Ti concentration in the ternary U-As-Cu and U-As-Ti system keeping the ratio [U]/[As] fixed. Solid lines are to guide the eye. (A)–(D) denote the ratio [U]/[As] and are indicated as vertical lines on the left. The error bars denote the deviation in the ratio [U]/[As] where applicable. Compositions of U-As, U-As-Cu, and U-As-Ti are listed in the caption of Fig. 2.

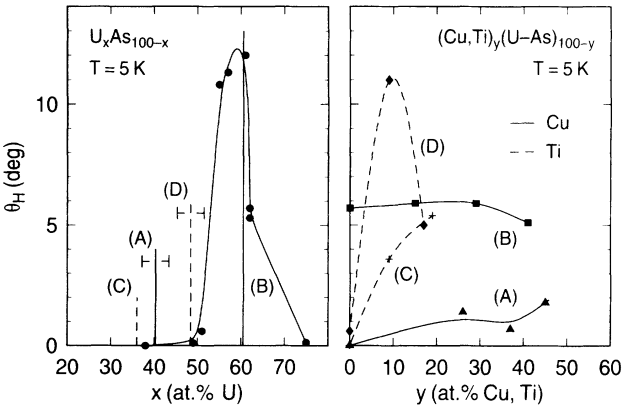

FIG. 5. The Hall angle θ_H as a function of U concentration for the binary U-As system and (right) as a function of Cu and Ti concentration in the ternary U-As-Cu and U-As-Ti system keeping the ratio [U]/[As] fixed. Solid lines are to guide the eye. (A)–(D) denote the ratio [U]/[As] and are indicated as vertical lines of the left. The error bars denote the deviation in the ratio [U]/[As] where applicable. Compositions of U-As, U-As-Cu, and U-As-Ti are listed in the caption of Fig. 2.

The Hall angle θ_H is plotted in Fig. 5. For the binary U_xAs_{100-x} system (Fig. 5 left) θ_H follows the same compositional dependence as T_C or M_U with a maximum value of 12° at $x \simeq 60$. Adding Cu (set A and B in Fig. 5 right) does not change θ_H considerably even for low [U]/[As] ratio where M_U is strongly increased (set A in Fig. 2 right). Adding Ti (set C and D in Fig. 5 right), on the other hand, increases θ_H more than adding Cu reaching 11° in $U_{42}As_{49}Ti_{09}$.

Figure 6 depicts the polar Kerr rotation of the U-As system at a temperature of 10 K and in a field of 3 T. The photon energy range is limited to 3.5 eV due to the increasing absorption of the glass substrate. The Kerr rotation does not saturate completely even in fields up to 7 T as seen in the Kerr-rotation loop shown in Fig. 7. The largest rotation is measured in the $U_{61}As_{39}$ film reaching

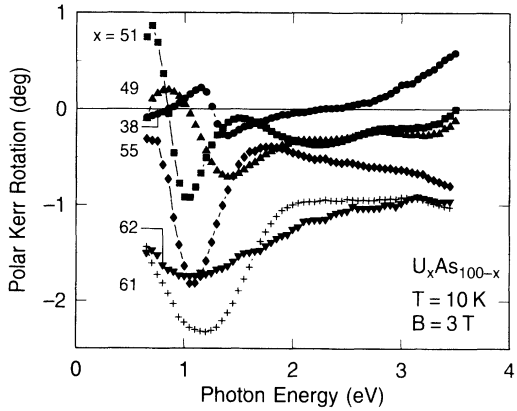

FIG. 6. The polar Kerr rotation for the U_xAs_{100-x} compositions with $x = 38$ (●), 49 (▲), 51 (■), 55 (◆), 61 (+), 62 (▼) as measured through the glass substrate. The data are taken at a temperature of 10 K and in a field of 3 T.

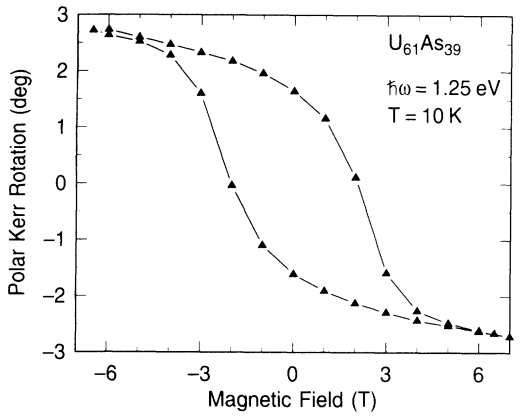

FIG. 7. The polar Kerr-rotation loop of $U_{61}As_{39}$ at a photon energy of 1.25 eV as measured through the glass substrate at a temperature of 10 K.

$-2.7°$ at 1.25 eV in a field of 7 T. This value is obtained by measuring through the substrate. Therefore, the rotation as seen directly on the film would be $-2.7°/1.4 \simeq -2°$, if we set the index of refraction of the substrate equal to 1.4 (see the Appendix). Looking at the energy spectra (Fig. 6) one notices that for U concentrations $x \geq 55$ the Kerr rotation is dominated by a broad negative peak around 1.2 eV as in crystalline UAs.[2] At $x < 55$ the negative peak narrows and decreases in size. In addition, a positive peak appears below 1 eV. It has been pointed out before[9] that the appearance of the positive peak, which has a much higher coercivity and remanence than the negative peak in the same film, can be explained with a phase separation into an amorphous metallic UAs phase and an amorphous semiconducting UAs_2 phase. A positive peak in the compositions with low U concentration is confirmed in the paramagnetic $U_{38}As_{62}$ film as shown in Fig. 6.

The polar Kerr rotation of the U-As-Cu system is plotted at 10 K and 3 T in Fig. 8. The spectra for the films

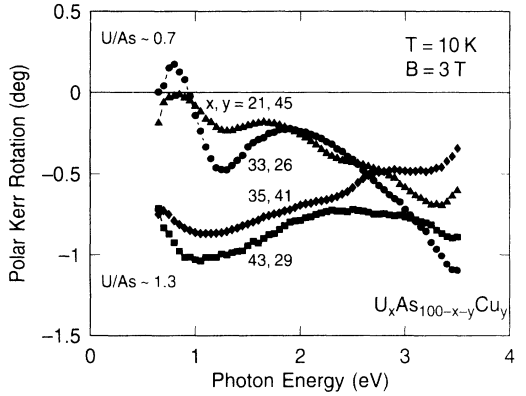

FIG. 8. The polar Kerr rotation for the U-As-Cu system with ratio $[U]/[As] \simeq 0.7$ $U_{21}As_{34}Cu_{45}$ (▲), $U_{33}As_{41}Cu_{26}$ (●), and with ratio $[U]/[As] \simeq 1.3$ $U_{35}As_{23}Cu_{41}$ (◆), $U_{43}As_{28}Cu_{29}$ (■) as measured through the glass substrate. The data are taken at a temperature of 10 K and in a field of 3 T.

with a high ratio $[U]/[As] \simeq 1.3$ resemble very much the spectra for the U_xAs_{100-x} films with $x \geq 55$. They are dominated by a broad negative peak near 1 eV. The maximum rotation is much lower as compared to U_xAs_{100-x} and reaches $-1.05°$ at 1.05 eV in $U_{43}As_{28}Cu_{29}$. In the films with low ratio $[U]/[As] \simeq 0.7$ a positive peak appears below 1 eV indicating a second phase as in U_xAs_{100-x} with $x < 55$. The resistivity data (set A and B in Fig. 4 right), however, do not show a transition into a semiconducting phase.

The last system investigated, U-As-Ti, is shown in Fig. 9, where the polar Kerr rotation is plotted at 10 K and 3 T. All spectra are dominated by a broad negative peak between 1.2 and 1.8 eV. Maximum Kerr values are higher than in the U-As-Cu system, reaching $-1.45°$ at 1.3 eV in $U_{42}As_{49}Ti_{09}$. There is no indication of a positive peak and, hence, no second phase as seen in the binary U-As and in the ternary U-As-Cu films.

DISCUSSION

The binary U_xAs_{100-x} system orders ferromagnetically in the composition range $49 \leq x \leq 75$ as shown in Fig. 3. The upper limit is probably due to the increasing delocalization of the U $5f$ states as one approaches the limit of metallic uranium.[16] The lower limit, however, seems to be connected with an increase in resistivity (Fig. 4 left). As shown previously,[9] this increase can be understood in terms of a phase separation into a metallic UAs and a semiconducting UAs_2 amorphous phase. As a consequence of the resistivity increase, the strength of the RKKY exchange interaction, which depends on the presence of charge carriers, is decreased. Adding Cu to the U-As system in a range where the metallic amorphous UAs phase prevails (set B in Figs. 2 and 3) keeps M_U and even T_C constant. Although the U atoms are diluted and their average separation increased, the strength of the exchange, as reflected in the high T_C, is partially maintained. Adding Cu in a region where the semiconducting amorphous phase is present (set A) strongly increases M_U, which reaches values as large as the largest values in the binary U-As system. It has to be pointed out that M_U is averaged over the total amount of U atoms in both phases because there is no way to separate M_U for each phase. T_C, however, reaches only half the maximum value of U-As indicating a weaker exchange. Another interesting fact can be seen from the Kerr spectra (Fig. 8). The samples with low ratio $[U]/[As] \simeq 0.7$ show the signature of a second amorphous phase as in the binary U-As system,[9] whereas the ones with high ratio $[U]/[As] \simeq 1.3$ do not. Thus the addition of Cu in samples with a low $[U]/[As]$ ratio does not prevent a phase separation. But by providing additional charge carriers the RKKY exchange is enhanced and the second phase, which is semiconducting in U-As, becomes conducting and shows ferromagnetic ordering.

The effect of Cu doping is best shown in a ternary diagram. Figure 10 depicts the ternary diagram in the U-As-Cu system for M_U and Fig. 11 for T_C. The known crystalline compounds are indicated by squares. In both figures the region of high ordering temperature and large

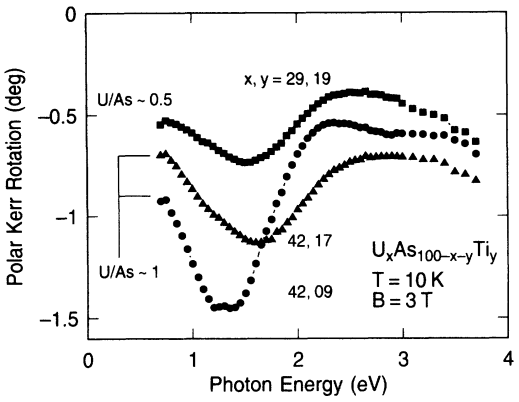

FIG. 9. The polar Kerr rotation for the U-As-Ti system with ratio [U]/[As]$\simeq$0.5 $U_{29}As_{52}Ti_{19}$ (■), and with ratio [U]/[As]$\simeq$1 $U_{42}As_{41}Ti_{17}$ (▲), $U_{42}As_{49}Ti_{09}$ (●) as measured through the glass substrate. The data are taken at a temperature of 10 K and in a field of 3 T.

magnetization is a ridge that stretches along a fixed ratio [U]/[As], i.e., on a straight line connecting the binary U-As axis with the Cu point. A plateau of large values of M_U is found in the center of the diagram near the crystalline UCu_2As_2 compound. The samples (open circles), which show the magneto-optical signature of a second phase, are all in the left half of the diagram.

The above considerations lead to the following picture of the influence of Cu addition to the U-As system: In the binary U_xAs_{100-x} system two phases can be distinguished which show a typical spectral dependence of

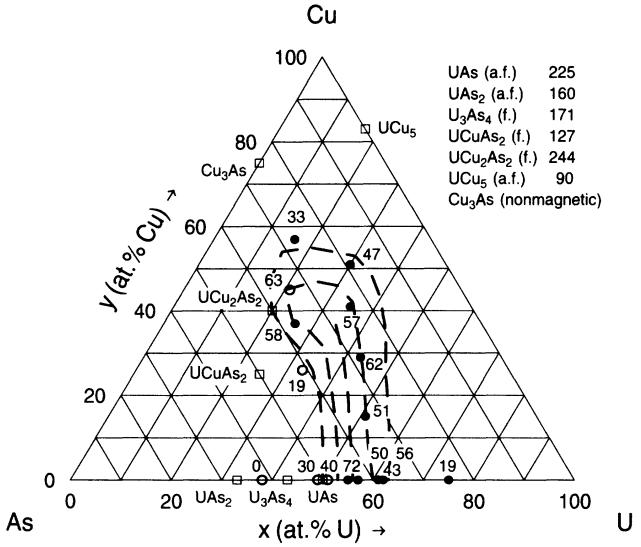

FIG. 10. The magnetization per U atom for the ternary U-As-Cu system. The values are given in $10^{-2}\mu_B$/U. Open circles are compositions that show indication of a second phase in the Kerr spectra. Crystalline compounds are indicated by squares and their values (from Refs. 2, 10, 12, and 17) are given in the table inset. (a.f.) means antiferromagnet and (f.) means ferromagnet.

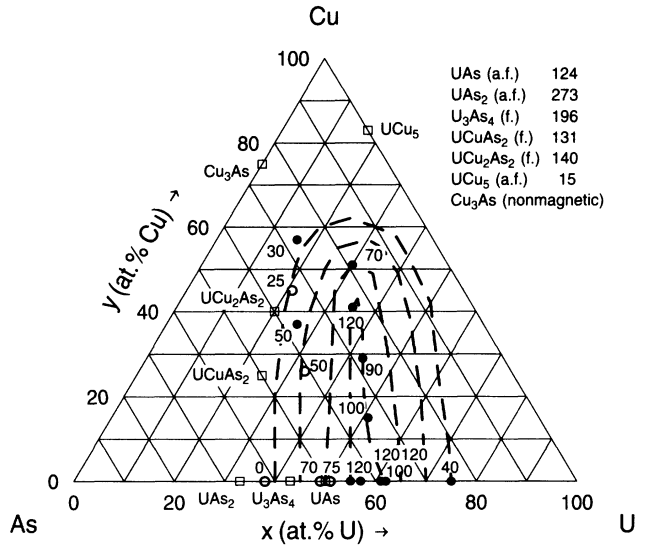

FIG. 11. The Curie temperature for the ternary U-As-Cu system. The values are given in Kelvin. Open circles are compositions that show indication of a second phase in the Kerr spectra. Crystalline compounds are indicated by squares and the values (from Refs. 2, 10, 12, and 17) of the Curie or Néel (for antiferromagnets) temperature are given in the table inset. (a.f.) means antiferromagnet and (f.) means ferromagnet.

the polar Kerr rotation. First, on the U-rich side a metallic phase with a NaCl-structure-like local coordination of the U atoms and, second, on the U-poor side a semiconducting phase with a Cu_2Sb-structure-like local coordination. Adding Cu does not change the local coordination of the U atoms, which seems to depend solely on the [U]/[As] ratio, but has mainly the effect of adding additional charge carriers thus enhancing the RKKY exchange interaction. This conclusion is corroborated by the fact that the amorphous composition $U_{35}As_{23}Cu_{41}$ with a ratio [U]/[As]$\simeq$1.3 shows a NaCl-structure-like Kerr spectrum although the U concentration is in a range where the binary U-As system shows a Cu_2Sb-structure-like Kerr spectrum. $U_{33}As_{41}Cu_{26}$, on the other hand, with a ratio [U]/[As]$\simeq$0.7 shows a Cu_2Sb-structure-like Kerr rotation although it has similar U concentration.

The effects of Ti doping seem at first similar to Cu doping, however, a ternary diagram reveals some fundamental differences. Figures 12 and 13 show M_U and T_C, respectively, of the U-As-Ti amorphous system. In contrast to the U-As-Cu system, the region of large M_U and high T_C does not follow a line of constant [U]/[As] ratio, but it rather curves towards the As-rich side of the diagram. In addition, the region is considerably smaller than in the U-As-Cu system. A further difference is that all the Kerr spectra show a NaCl-structure-like energy dependence (Fig. 9) and there is no magneto-optical evidence for a second phase even at ratios [U]/[As]$\simeq$0.5. This indicates that Ti, besides adding charge carriers, is changing the local coordination of the U atoms. The [U]/[As] ratio appears to be shifting to the U-rich side. Considering that Ti is a very reactive metal, it is conceiv-

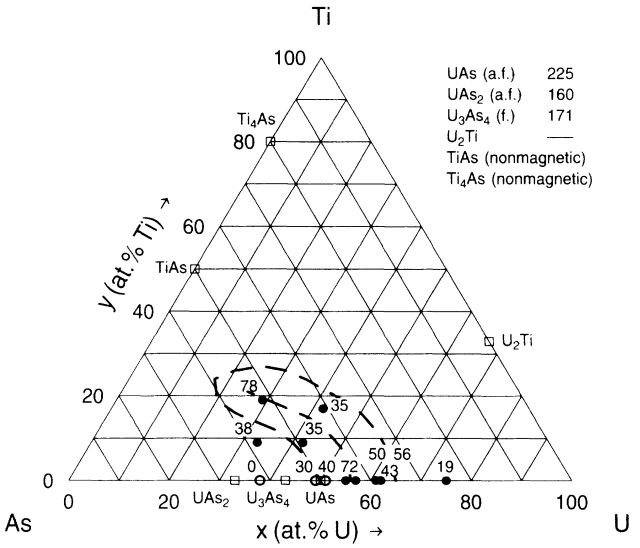

FIG. 12. The magnetization per U atom for the ternary U-As-Ti system. The values are given in $10^{-2}\mu_B$/U. Open circles are compositions that show indication of a second phase in the Kerr spectra. Crystalline compounds are indicated by squares and their values (from Refs. 2, 10, 12, and 17) are given in the table inset. (a.f.) means antiferromagnet and (f.) means ferromagnet. The magnetic properties of U_2Ti are not known.

able that Ti binds As much stronger than Cu does. It may even form a nonmagnetic Ti-As phase, therefore taking away As from the U environment and preventing the formation of a Cu_2Sb-structure-like phase. The NaCl-structure-like Kerr spectrum of $U_{29}As_{52}Ti_{19}$, as pictured

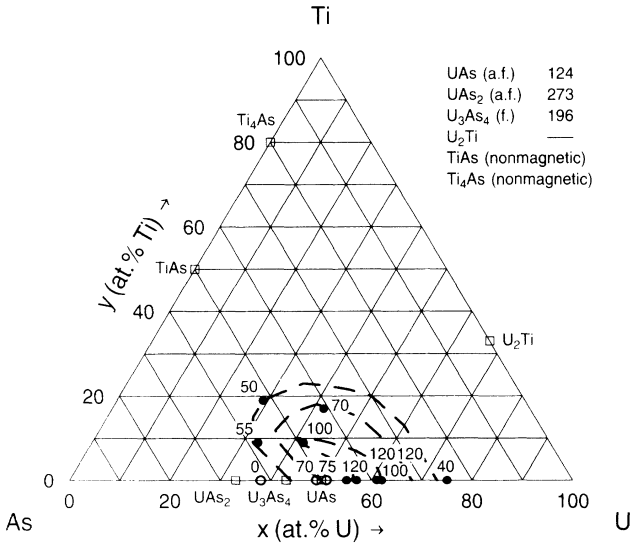

FIG. 13. The Curie temperature for the ternary U-As-Ti system. The values are given in Kelvin. Open circles are compositions that show indication of a second phase in the Kerr spectra. Crystalline compounds are indicated by squares and the values (from Refs. 2, 10, 12, and 17) of the Curie or Néel (for antiferromagnets) temperature are given in the table inset. (a.f.) means antiferromagnet and (f.) means ferromagnet. The magnetic properties of U_2Ti are not known.

in Fig. 9, gives strong evidence for this conclusion.

Besides the magnetic properties it is worthwhile to discuss the magnitude of the polar Kerr effect in the binary U-As and the ternary U-As-Cu and U-As-Ti system and compare it to the values obtained on crystalline compounds. The two binary crystalline compounds investigated are UAs (NaCl structure) and U_3As_4 (Th_3P_4 structure).[2] The polar Kerr spectra are due to fundamentally different transitions. In UAs the dominating transition is an interband transition from rather localized U $5f$ states into the U $6d$ derived conduction band. In U_3As_4, however, the Kerr spectra originate from an intraband transition of highly spin-polarized charge carriers within the conduction band. As a consequence, the Kerr rotation of UAs shows a broad negative peak at 1.4 eV and in U_3As_4 there is no peak but a sharp increase of the negative Kerr rotation towards lower energies.[2] The similarity of the Kerr spectra in U_xAs_{100-x}, where $x \geq 55$, with the spectrum of crystalline UAs has led us to assign the peak to a U $5f \rightarrow 6d$ transition.

To compare the Kerr rotations of different U compositions we scale the absolute value of the peak Kerr rotation with the index of refraction of glass, $n_s = 1.4$, to account for the enhancement due to measuring through the glass substrate. Furthermore, we scale with the magnetization per U atom, M_U, and with the number of U atoms per cm^3, N_U, which is calculated from the atomic volumes and the chemical analysis. This procedure is appropriate because the Kerr effect is proportional to the magnetization and, for a given electronic transition, to the number of atoms contributing to that transition. The scaled absolute peak values $\Theta_K = \theta_{Ks}(E_{pk})/n_s M_U N_U$ are listed in Table I, where $\theta_{Ks}(E_{pk})$ is the value of the Kerr rotation at the peak energy E_{pk}. For comparison, the values for UAs (Ref. 2) and $UCuAs_2$ (Ref. 13) are listed as well. It is evident that the scaled Kerr rotations Θ_K are almost equal in the two crystalline compounds despite the large difference in Kerr rotation. This mainly indicates that the Kerr rotation originates from the same type of transition (U $5f \rightarrow 6d$) with comparable joint spin polarization, bandwidth, and radial overlap of the wave functions of initial and final states. It has to be pointed out that such a scaling is usually done with the off-diagonal conductivity $\tilde{\sigma}_{xy}$, which is a property independent of the optical functions $n(\omega)$ and $k(\omega)$. For the Kerr rotation such a scaling is only appropriate under the assumption that the optical functions $n(\omega)$ and $k(\omega)$ are similar in size and the maximum Kerr rotation occurs at approximately the same energy. Because the reflectivity spectra of UAs (Ref. 1) and $UCuAs_2$ (Ref. 13) are comparable in the energy range of the peak rotation, the scaling gives to first order a reasonable value for the strength of the transition. The reflectivity spectra for the binary and ternary amorphous films are rather featureless and of the same size. Hence, the differences due to varying optical functions should not be too large.

Looking at the binary U_xAs_{100-x} system (Table I), we note that the values of Θ_K form two groups. For $x > 55$, Θ_K is of equal size as in the crystalline materials. This is also the composition range where the polar Kerr spectra

TABLE I. Magnetic and magneto-optical properties of amorphous U-As and U-As-Cu and U-As-Ti films. E_{pk} is the energy of the peak Kerr rotation. $\theta_{Ks}(E_{pk})$ is the peak Kerr rotation as measured through the substrate and $\theta_K(E_{pk})$ is the peak Kerr rotation as measured from the film side. M_U is the magnetization per U atom, N_U is the number of U atoms per cm^3, and Θ_K is $\theta_K(E_{pk})$ divided by M_U and N_U.

Composition	E_{pk} (eV)	$\theta_{Ks}(E_{pk})$ (deg)	$\theta_K(E_{pk})$ (deg)	M_U (μ_B/U)	N_U (10^{22} cm^{-3})	Θ_K (10^{-22} cm^3 deg μ_B^{-1})
UAs (cryst.)	1.45		−1.05	0.42	2.08	1.2
$UCuAs_2$ (cryst.)	1.2		−1.75	1.27	1.34	1.03
$U_{49}As_{51}$	1.4	−0.7	−0.5	0.3	2.31	0.72
$U_{51}As_{49}$	1.05	−0.9	−0.65	0.4	2.41	0.67
$U_{55}As_{45}$	1.1	−1.8	−1.3	0.72	2.6	0.69
$U_{61}As_{39}$	1.2	−2.3	−1.65	0.5	2.92	1.13
$U_{62}As_{38}$	1.1	−1.7	−1.2	0.43	2.93	0.95
$U_{21}As_{34}Cu_{45}$	1.3	−0.25	−0.2	0.63	1.24	0.26
$U_{33}As_{41}Cu_{26}$	1.3	−0.5	−0.35	0.19	1.75	1.05
$U_{35}As_{24}Cu_{41}$	1.1	−0.8	−0.55	0.57	2.04	0.47
$U_{43}As_{28}Cu_{29}$	1.05	−1.05	−0.75	0.62	2.34	0.52
$U_{29}As_{52}Ti_{19}$	1.5	−0.7	−0.5	0.77	1.41	0.46
$U_{42}As_{41}Ti_{17}$	1.6	−1.2	−0.85	0.32	2.04	1.3
$U_{42}As_{49}Ti_{09}$	1.35	−1.45	−1.05	0.32	2.01	1.63

have similar shape as crystalline UAs (Fig. 6). The maximum Kerr response is reached in samples with 60 at. % U and it is of similar strength as in crystalline UAs. For $x \leq 55$, Θ_K is reduced by a factor of 2 probably through the presence of a semiconducting second phase, which was mentioned before. The reason for a reduction might be found in a smaller radial overlap integral of the U $5f$ and $6d$ wave functions. A broadening effect, however, can be ruled out as the negative peaks even narrow at low U concentrations (see Fig. 6).

The U-As-Cu system has very small values of Θ_K (Table I) with the exception of one composition, $U_{33}As_{41}Cu_{26}$, where the magnetization is very small. The reasons for the smaller values of Θ_K in the samples with ratio [U]/[As]$\simeq$1.3 as compared to the binary U-As system with similar [U]/[As] ratio are not clear. All magnetic and transport properties remain constant upon adding Cu to the binary U-As system. The small values for Θ_K might be connected with changes in the structure of the conduction band that lead to either a reduced overlap integral of the U $5f$ and $6d$ wave functions or a change in the matrix element of the U $5f \rightarrow 6d$ transition.

The values of Θ_K (Table I) for the U-As-Ti system with ratio [U]/[As]$\simeq$1 are even higher than in the binary U-As films, whereas Θ_K for U-As-Ti films with ratio [U]/[As]$\simeq$0.5 is equal in value to U-As-Cu films with high [U]/[As] ratio. As has been discussed before, the Ti seems to change the local coordination of the U atom to a NaCl-structure-like coordination which is the range of U-U interatomic distance where the U $5f \rightarrow 6d$ transition is strongest in the binary U-As system. Because of its high valence, Ti is likely to add charge carriers. But the changes in the conduction band associated therewith do not suppress the strength of the U $5f \rightarrow 6d$ transition as is the case in the U-As-Cu system.

CONCLUSIONS

The spectral dependence of the polar Kerr rotation in the amorphous U_xAs_{100-x} system is dominated by a broad negative peak for U concentrations $x \geq 55$ similar to the spectrum of the crystalline UAs compound. At $x < 55$ phase separation into two amorphous phases occurs, which is indicated by the appearance of a positive peak below 1 eV in the Kerr spectra. In the amorphous U-As-Cu system, for compositions with a low ratio [U]/[As]$\simeq$0.7 the polar Kerr spectra indicate the onset of a similar phase separation. No such indication is found, however, in the amorphous U-As-Ti system for the composition range investigated.

It is concluded that the addition of Cu to U-As does not change the local coordination of the U atoms. It adds additional electrons which enhance the RKKY exchange interaction allowing magnetic order even at low U concentrations. The addition of Ti to U-As changes the local coordination of the U atom presumably because Ti binds As due to its reactivity. This has the effect that the local coordination of the U atoms is like the NaCl structure even for low [U]/[As] ratio. The additional electrons provided by the Ti also increase the RKKY interaction leading to magnetic order at low U concentrations. However, this study shows that adding electrons does not increase T_C beyond the value of the binary amorphous U films or the crystalline U compounds. This result suggests that the RKKY interaction is not the dominating interaction in amorphous U materials and that a room-temperature T_C cannot be achieved in amorphous U films by means of the RKKY interaction.

A scaling law applied to the maximum polar Kerr rotation indicates that the strength of the U $5f \rightarrow 6d$ transition, which is responsible for the magneto-optical

response, is the same as in the crystalline compounds. Therefore, the disorder of the amorphous state does not seem to harm the magneto-optical response. This suggests that amorphous thin films are suitable to study the compositional dependence of the Kerr effect and the influence of the addition of other elements on the Kerr effect.

ACKNOWLEDGMENTS

The authors thank M. M. Plechaty for the chemical analysis and J. M. Karasinski and J. M. Rigotty for technical assistance.

APPENDIX: INFLUENCE OF THE SUBSTRATE ON THE KERR EFFECT

In order to understand the influence of the substrate on the Kerr effect one has to derive the relation between the complex polar Kerr effect, $\tilde{\phi}_{Ks}=\theta_{Ks}-i\varepsilon_{Ks}$, where θ_{Ks} is the polar Kerr rotation and ε_{Ks} is the polar Kerr ellipticity, and the off-diagonal conductivity $\tilde{\sigma}_{xy}=\sigma_{1xy}+i\sigma_{2xy}$ in the case of a substrate–magnetic-medium interface. The reflection coefficient $\tilde{\rho}$ for electromagnetic radiation under near-normal incidence on an absorbing medium with complex index of refraction $\tilde{n}=n-ik$, where n is the index of refraction and k is the absorption coefficient, facing vacuum is given by

$$\tilde{\rho}=\frac{\tilde{n}-1}{\tilde{n}+1} . \tag{A1}$$

If the same medium is facing a transparent substrate with real index of refraction n_s the reflection coefficient is defined as

$$\tilde{\rho}_s=\frac{\tilde{n}-n_s}{\tilde{n}+n_s} . \tag{A2}$$

In the case of a magneto-optically active material the complex reflection coefficient and, therefore, the complex index of refraction, are different for right (+) and left (−) circular polarized light. For θ_{Ks}, $\varepsilon_{Ks}\ll 1$ rad the complex polar Kerr effect is then expressed as

$$\tilde{\phi}_{Ks}=i\frac{\tilde{\rho}_{s+}-\tilde{\rho}_{s-}}{\tilde{\rho}_{s+}+\tilde{\rho}_{s-}} . \tag{A3}$$

Inserting Eq. (A2) into (A3) yields

$$\tilde{\phi}_{Ks}=i\frac{n_s(\tilde{n}_+-\tilde{n}_-)}{\tilde{n}_+\tilde{n}_--n_s^2} . \tag{A4}$$

Using $\tilde{\varepsilon}_\pm=\tilde{n}_\pm^2$, where $\tilde{\varepsilon}_\pm=\tilde{\varepsilon}_{xx}\mp i\tilde{\varepsilon}_{xy}$, and $\tilde{\varepsilon}_{ij}=\delta_{ij}-(4\pi i/\omega)\tilde{\sigma}_{ij}$, where $\tilde{\varepsilon}_{ij}=\varepsilon_{1ij}-i\varepsilon_{2ij}$ and $\tilde{\sigma}_{ij}=\sigma_{1ij}+i\sigma_{2ij}$, one gets

$$\tilde{\phi}_{Ks}=-\frac{4\pi i}{\omega}\frac{n_s\tilde{\sigma}_{xy}}{\tilde{n}(\tilde{n}^2-n_s^2)} , \tag{A5}$$

with $\tilde{n}=\frac{1}{2}(\tilde{n}_++\tilde{n}_-)$, the mean complex index of refraction. Separating real and imaginary parts in Eq. (A5) yields for the Kerr rotation and ellipticity

$$\theta_{Ks}=\frac{4\pi}{\omega}\frac{B_s\sigma_{1xy}+A_s\sigma_{2xy}}{A_S^2+B_s^2} \tag{A6}$$

and

$$\varepsilon_{Ks}=\frac{4\pi}{\omega}\frac{A_s\sigma_{1xy}-B_s\sigma_{2xy}}{A_s^2+B_s^2} . \tag{A7}$$

A_s and B_s are given by

$$A_s=(1/n_s)(n^3-3nk^2-n_s^2n) \tag{A8}$$

and

$$B_s=(1/n_s)(-k^3+3n^2k-n_s^2k) , \tag{A9}$$

where n and k are the mean index of refraction and absorption. Setting $n_s=1$ recovers the equations for a magneto-optically active material facing vacuum. The off-diagonal conductivity $\tilde{\sigma}_{xy}$ is independent of the interface. Thus, Eqs. (A6) and (A7) show that the polar Kerr effect is generally enhanced by a factor equivalent to the index of refraction n_s of the substrate.

[1] J. Schoenes, Phys. Rep. **66**, 187 (1980).

[2] W. Reim and J. Schoenes, in *Handbook of Ferromagnetic Materials,* edited by K. H. J. Buschow and E. P. Wolfarth (North-Holland, Amsterdam, 1990), Vol. 5, p. 133.

[3] W. Reim, J. Magn. Magn. Mater. **58**, 1 (1986).

[4] J. Schoenes, M. Küng, R. Hauert, and Z. Henkie, Solid State Commun. **47**, 23 (1983).

[5] P. P. Freitas and T. S. Plaskett, Phys. Rev. Lett. **64**, 2184 (1990).

[6] R. J. Gambino, T. S. Plaskett, T. R. McGuire, and M. W. McElfresh, J. Appl. Phys. **69**, 4750 (1991).

[7] T. R. McGuire, R. J. Gambino, M. W. McElfresh, and T. S. Plaskett, IEEE Trans. Magn. **26**, 1349 (1990).

[8] T. S. Plaskett, T. R. McGuire, P. Fumagalli, R. J. Gambino, and N. A. Bojarczuk, J. Appl. Phys. **70**, 5855 (1992).

[9] P. Fumagalli, R. J. Gambino, T. S. Plaskett, and T. R. McGuire, Appl. Phys. Lett. **60**, 258 (1992).

[10] Z. Zołnierek, D. Kaczorowski, R. Troć, and H. Noël, J. Less-Common. Met. **121**, 193 (1986).

[11] P. Fumagalli, J. Schoenes, and D. Kaczorowski, Solid State Commun. **65**, 173 (1988).

[12] P. Fumagalli, J. Schoenes, H. Rüegsegger, and D. Kaczorowski, Helv. Phys. Acta **61**, 829 (1988).

[13] J. Schoenes, P. Fumagalli, H. Rüegsegger, and D. Kaczorowski, J. Magn. Magn. Mater. **81**, 112 (1989).

[14] T. R. McGuire, T. S. Plaskett, P. Fumagalli, R. J. Gambino, N. A. Bojarczuk, and B. E. Argyle, J. Magn. Magn. Mater. (to be published).

[15] L. J. van der Pauw, Phillips Res. Rep. **13**, 1 (1958).

[16] H. H. Hill, in *Plutonium 1970,* edited by W. M. Miner (Met. Soc. AIME, New York, 1970), p. 2.

[17] J. M. Fournier, in *Actinides—Chemistry and Physical Properties,* edited by L. Manes (Springer, Berlin, 1985), p. 127.